

Research Article

Dynamic and Static Properties of Aqueous NaCl Solutions at 25°C as a Function of NaCl Concentration: A Molecular Dynamics Simulation Study

Song Hi Lee 

Chemistry Institute for Functional Materials, Pusan National University, Pusan, Republic of Korea

Correspondence should be addressed to Song Hi Lee; songhilee@pusan.ac.kr

Received 20 October 2020; Revised 11 November 2020; Accepted 23 November 2020; Published 9 December 2020

Academic Editor: Bryan M. Wong

Copyright © 2020 Song Hi Lee. This is an open access article distributed under the Creative Commons Attribution License, which permits unrestricted use, distribution, and reproduction in any medium, provided the original work is properly cited.

We present the result of molecular dynamics (MD) simulations to calculate the molar conductivity $\Lambda_m (= \lambda_{Na^+} + \lambda_{Cl^-})$ of NaCl in SPC/E water at 25°C as a function of NaCl concentration (c) using Ewald sums employing a velocity Verlet algorithm. It is found that the MD result for Λ_m with Ewald sum parameter $\kappa = 0.10 \text{ \AA}^{-1}$ gives the closest one to the experimental data and that the obtained radial distribution functions $g_{ij}(r)$ with $\kappa = 0.10 \text{ \AA}^{-1}$ show a dramatic change with a very deep minimum of $g_{NaCl}(r)$ and, as a result, sharp maxima of $g_{NaNa}(r)$ and $g_{ClCl}(r)$ at the distance 9.95 Å, which indicates a characteristic of ionic atmosphere, the basis of the Debye–Hückel theory of ionic solutions. The static and dynamic properties of NaCl (aq) solutions are analyzed in terms of radial distribution functions, hydration numbers, coordination numbers around Na^+ and Cl^- , residence times of water around Na^+ and Cl^- , water diffusion, and ion-ion electrostatic energies to explain the behavior of the molar conductivity Λ_m of NaCl obtained from our MD simulations.

1. Introduction

The theory that an electrolyte is dissolved in water and dissociated into ions was proposed by Arrhenius (Arrhenius's theory of electrolytic dissociation), who won the Nobel Prize in Chemistry in 1903, in his doctoral degree in 1884. Before this theory was raised, it was well known that a solution dissolved in an electrolyte passes electricity, and Faraday explained that the electrolyte dissolved in water is decomposed into charged ions by the action of this electricity. By measuring the molar electrical conductivity according to the concentration of various salt solutions, Kohlrausch obtained the relation (equation (1)) between the molar conductivity (Λ_m) and the molar concentration (c) of a strong electrolyte (Kohlrausch's law), and he found that each ion moved independently in an electric field. In the case of an electrolyte dissolved in a solvent and dissociated into ν_+ cations and ν_- anions, the limiting molar conductivity (Λ_m^o) in an infinitely dilute solution is related to the

limiting molar conductivity (λ_+^o and λ_-^o) of each ion, as shown in equation (2) (Kohlrausch's law of the independent migration of ions).

$$\Lambda_m = \Lambda_m^o - Kc^{1/2}, \quad (1)$$

where K is a constant.

$$\Lambda_m^o = \nu_+ \lambda_+^o + \nu_- \lambda_-^o, \quad (2)$$

where the limiting molar conductivities of Na^+ and Cl^- at 25°C are measured as 5.01 and 7.63 $\text{mS m}^2 \text{mol}^{-1}$ experimentally [1].

In 1925, Onsager extended the Debye–Hückel theory of electrolyte solutions, published two years ago, to come up with the Debye–Hückel–Onsager theory, which became an integral part of his Nobel Prize winning achievements. Around some ions, ions with opposite charges are surrounded by electrostatic forces. In the absence of an external electric field, the distribution of counter ions around the central ion is symmetric. However, when the electric field

acts, the ions at the center and the ions around them receive forces in opposite directions to create an asymmetric ionic atmosphere, and thereby, an electrostatic force acts in the direction opposite to the direction in which the ions move. The higher the concentration of the electrolyte, the greater this effect becomes, and thus, the molar conductivity becomes less than in a dilute solution. This reduction of the ions' molar conductivity is called the relaxation effect.

Another effect of the ionic atmosphere is the electrophoretic effect. Ions are hydrated with solvent molecules, and these solvent molecules move with the ions. Since the central ions and the surrounding ions move in opposite directions, the central ions move against the flow of the solvent moving together with the surrounding ions. Onsager took these two points into consideration and treated the ion motion as a zigzag Brownian motion rather than a straight line in the electric field and derived the following molar conductivity equation. The Debye–Hückel–Onsager theory is an attempt to obtain quantitative expressions which leads to a Kohlrausch-like expression:

$$\Lambda_m = \Lambda_m^0 - (A + B \Lambda_m^0) c^{1/2}, \quad (3)$$

where A and B are coefficients determined by temperature and the dielectric constant and viscosity of the solvent. The numerical values of A and B in water are $6.02 \text{ mS m}^2 \text{ mol}^{-1} (\text{mol} \cdot \text{L}^{-1})^{1/2}$ and $0.229 (\text{mol} \cdot \text{L}^{-1})^{1/2}$ [1]

A systematic conductivity study of sodium chloride-water + 1, 4-dioxane in dilute solutions ($c < 0.01 \text{ mol} \cdot \text{dm}^{-3}$) [2] has been conducted covering a broad solvent composition range at temperatures from 5 to 35°C. Accurate viscosity and permittivity data were determined for the organic solvent system. Evaluation of the limiting molar conductivity Λ^∞ , ionic conductivities Λ_+^∞ and Λ_-^∞ , and the association constant K_A is based on the chemical model [3] of electrolyte solutions, including short-range forces. In the next paper [4], they reported on an extension of this study to concentrated solutions, covering the temperature range from 5 to 35°C at a solvent mole fraction of dioxane from $x_D = 0$ to 0.65 and electrolyte concentration up to the limit of salt solubility in the respective mixtures and up to $5 \text{ mol} \cdot \text{dm}^{-3}$ in water. Data analysis is based on the mean spherical approximation (MSA) [5]. Comparison is made with the data representation by the empirical Casteel–Amis equation [6]. The association constants of the MSA are compared with those from chemical model calculations at low concentrations (lcCM). Later on, an investigation of ion-pairing of alkali metal halides in aqueous solutions using the electrical conductivity and the Monte Carlo computer simulation methods was reported. [7].

In our previous paper [8], we reported molecular dynamics (MD) simulations for the ionic mobilities μ of Na^+ and Cl^- ions, in the system of Na^+ (or Cl^-) ion + 1023 water molecules, at 25°C using reaction field correction (RFC), simple truncation (ST), and Ewald sums employing Gear's fifth order predictor-corrector and velocity Verlet algorithms. We found that MD simulations using Ewald sum with $\kappa = 0.20\text{--}0.30 \text{ \AA}^{-1}$ employing a velocity Verlet algorithm gives the best result for μ_{Na^+} and μ_{Cl^-} at 25°C, even though

the calculated μ_{Na^+} overestimates the experimental data and the μ_{Cl^-} underestimates them. This behavior of μ_{Na^+} is opposite to that reported in our other MD simulations [9].

In this study, we have carried out MD simulations to calculate the molar conductivity Λ_m of NaCl in SPC/E water at 25°C as a function of NaCl concentration (c) using Ewald sums employing a velocity Verlet algorithm. The primary goal of this study is to analyze radial distribution functions, hydration numbers, coordination numbers, residence times, and ion-ion electrostatic energies water diffusion to understand the behavior of the ionic atmosphere around Na^+ and Cl^- ions through our MD simulations. This paper is organized as follows: Section 2 contains a brief description of molecular models and MD simulation methods followed by Section 3, which presents the results of our simulations. Our conclusion is summarized in Section 4.

2. Molecular Models and Molecular Dynamics Simulation Details

In order to establish systems of electrolyte solution of NaCl for MD simulation, we consider a system of $c = 1$ molar concentration (mol/L) of NaCl solution with 36 of Na^+ and Cl^- ions at 25°C. Then, the volume of this solution is simply equal to $V = V_{\text{soln}} = 36000 \text{ cm}^3 / N_A$ with N_A , Avogadro's number, which is the fixed volume for all the current MD simulations of NaCl in electrolyte systems, which gives the length of simulation box $L = 39.1009 \text{ \AA}$. It is very hard to find the relation between the molar concentration (c) and the density of the solution (ρ_t , g/cm^3) of NaCl solution in the literature. Instead, we use the experimental data of the weight percent ($\%W_{\text{NaCl}}$) and the density (ρ_t , g/cm^3) of NaCl solutions (Table 1) to find the numbers of ions (N_{NaCl}) and water (N_w). First, the relationship between ρ_t and $\%W_{\text{NaCl}}$ is obtained by using the least squares method from Table 1.

$$\rho_t = 0.00758333853\%W_{\text{NaCl}} + 0.9942949 (\text{g}/\text{cm}^3). \quad (4)$$

For $c = 1 \text{ mol/L}$ of $N_{\text{NaCl}} = 36$ with $V = 36000 \text{ cm}^3 / N_A$,

$$\rho_t = (18.0152N_w + 36 \times 58.443) / 36000 (\text{g}/\text{cm}^3). \quad (5)$$

Also,

$$\%W_{\text{NaCl}} = (36 \times 58.443) / (18.0152N_w + (36 \times 58.443)) \times 100. \quad (6)$$

Substituting equations (5) and (6) into equation (4), we obtain $N_w = 1956$. Numbers of water molecules for given c are obtained using the same process and listed in Table 2.

The SPC/E model [10] was adopted for water-water and ion-water. The pair potential between water and ion has the TIPS form [11]:

$$v_{iw} = 4\epsilon_{io} \left[\left(\frac{\sigma_{io}}{r_{io}} \right)^{12} - \left(\frac{\sigma_{io}}{r_{io}} \right)^6 \right] + \sum_{j \in w} \frac{q_i q_j}{r_{ij}}, \quad (7)$$

where σ_{io} and ϵ_{io} are Lennard–Jones (LJ) parameters between oxygen on a water molecule and an ion i , q_j is the charge at site j in water, and q_i is the charge on ion i .

TABLE 1: Experimental data between %W_{NaCl} and ρ_t at 25°C. The relationship ($\rho_t = 0.00758333853 \text{ \%W}_{\text{NaCl}} + 0.9942949$) is obtained by using the least squares method.

%W _{NaCl}	1	2	4	6	8	10	12
ρ_t (g/cm ³)	1.00409	1.01112	1.02530	1.03963	1.05412	1.06879	1.08356
%W _{NaCl}	14	16	18	20	22	24	26
ρ_t (g/cm ³)	1.09872	1.11401	1.12954	1.14533	1.16140	1.17760	1.19443

TABLE 2: The MD simulated systems in this study.

System	Number of Na ⁺ (Cl ⁻) ion (s)	Number of molecules (N_w)	Number of water (mol/L)	%W _{NaCl}	ρ_t (g/cm ³)
A1	1	1986	0.0278	0.16308	0.99546
A2	2	1985	0.0556	0.32580	0.99658
A3	4	1984	0.111	0.64980	0.99933
A4	8	1981	0.222	1.29314	1.00432
A5	18	1972	0.5	2.87598	1.01605
A6	36	1956	1.0	5.63432	1.03727
A7	72	1918	2.0	10.8560	1.07670
A8	108	1875	3.0	15.7441	1.11362
A9	144	1828	4.0	20.3538	1.14854

Moreover, r_{io} and r_{ij} are the distances between ion i and an oxygen site of a water molecule and between ion i and a charge site j in water, respectively. The LJ parameters σ_{io} and ϵ_{io} between oxygen on an SPC/E water molecule and the Na⁺ or Cl⁻ ion i were fitted to the binding energies of small clusters of ions by Dang et al. ($\sigma_{OO} = 2.876 \text{ \AA}$, $\sigma_{NaO} = 2.876 \text{ \AA}$, $\sigma_{ClO} = 3.785 \text{ \AA}$, $\epsilon_{OO} = 0.6502 \text{ kJ/mol}$, and $\epsilon_{NaO} = \epsilon_{ClO} = 0.5216 \text{ kJ/mol}$) [12, 13]. The electrostatic charges of SPC/E water and ions are $q_{O^{2-}} = -0.8476e$, $q_{H^+} = 0.4238e$, $q_{Na^+} = 0.1e$, and $q_{Cl^-} = -0.1e$. The pair potential energy of ion-ion also has the TIPS form [11]:

$$v_{ij} = 4\epsilon_{ij} \left[\left(\frac{\sigma_{ij}}{r_{ij}} \right)^{12} - \left(\frac{\sigma_{ij}}{r_{ij}} \right)^6 \right] + \frac{1}{2} \sum_{j \neq i} \frac{q_i q_j}{r_{ij}}, \quad (8)$$

where σ_{ij} and ϵ_{ij} are Lennard-Jones (LJ) parameters between ion i and ion j , q_i is the charge on ion i , and r_{ij} is the distance between ion i and ion j . The LJ parameters σ_{ij} and ϵ_{ij} between ion i and ion j are given by $\sigma_{NaNa} = 2.583 \text{ \AA}$, $\sigma_{ClCl} = 4.401 \text{ \AA}$, $\sigma_{NaCl} = 3.492 \text{ \AA}$, and $\epsilon_{NaNa} = \epsilon_{ClCl} = \epsilon_{NaCl} = 0.4184 \text{ kJ/mol}$ [12, 13]. Recently, even though many new models including Lennard-Jones parameters and the electrostatic charges of ions for aqueous electrolyte solutions have been developed [14–16], we have used the SPC/E model for water-water and ion-water, equation (7), since this model was used in our previous studies with and without Ewald sums [8, 12, 17].

Each MD simulation was carried out in the canonical ensemble (NVT fixed), and the density of NaCl solution is given in Table 1, which corresponds to a cubic box length of $L = 39.1009 \text{ \AA}$ for all the MD simulations. The usual periodic boundary condition in the x-, y-, and z-direction and the minimum image convention for pair potential were applied. Gaussian kinetics [18, 19] was used to control the temperature, and a quaternion formulation [20, 21] was employed to solve the equations of rotational motion about

the center of mass of rigid SPC/E water molecules. We have employed a velocity Verlet algorithm [22] for the time-integration algorithms: with a time step of 1 femtosecond.

For the Ewald sums, the Ewald sum parameters κ are varied from 0.05 to 0.25 \AA^{-1} in 0.05 \AA^{-1} increments, and the cutoff sphere of radius R_c in the real space and k_{max} in the reciprocal space are chosen as $L/2$ and 7, but $|k|^2 \leq 27$. MD runs of 500,000 time steps each were needed for the ion-water system to reach equilibrium. The equilibrium properties were then averaged over 10 blocks of 100,000 time steps (0.1 ns) for a total of 1,500,000 (1.5 ns) for the systems of given 5 values of κ and given 9 molar concentrations (mol/L). The configurations of water molecules and Na⁺ (Cl⁻) ion(s) were stored every 5 time steps for further analysis.

There are two routes to calculate self-diffusion coefficients of water from MD simulations: the Einstein relation from the mean square displacement (MSD),

$$D_i = \frac{1}{6} \lim_{t \rightarrow \infty} \frac{d}{dt} \langle [r_i(t) - r_i(0)]^2 \rangle, \quad (9)$$

and the Green-Kubo (GK) relation from the velocity autocorrelation (VAC) function,

$$D_i = \frac{1}{3} \int_0^\infty dt \langle v_i(0) \cdot v_i(t) \rangle. \quad (10)$$

3. Results and Discussion

3.1. Diffusion Coefficient. D_{Na^+} and D_{Cl^-} at 25°C in SPC/E water were obtained from mean square displacements (MSDs), equation (9), of Na⁺ and Cl⁻ from our MD simulations using Ewald sum with $\kappa = 0.05\text{--}0.25 \text{ \AA}^{-1}$ employing a velocity Verlet algorithm. We have listed sum of Na⁺ and Cl⁻ diffusion coefficients $D (= D_{Na^+} + D_{Cl^-})$ in Table 3 and compared D as a function of molar concentration (c) of NaCl with the experimental data [23] in Figure 1. Figure 1 shows

TABLE 3: Diffusion coefficients (D , $10^{-9} \text{ m}^2 \cdot \text{sec}^{-1}$) of NaCl in SPC/E water at 25°C employing a velocity Verlet algorithm, where n is the number of (Na^+ or Cl^-) ion(s).

System (n)	$\kappa = 0.05$	$\kappa = 0.10$	$\kappa = 0.15$	$\kappa = 0.20$	$\kappa = 0.25$	Best to exp.	(κ , \AA^{-1})
A1 (1)	5.73	5.06	5.08	4.56	4.61	A1 (0.25)	4.61
A2 (2)	4.65	3.85	3.82	3.94	3.73	A2 (0.25)	3.73
A3 (4)	3.91	3.46	3.64	3.47	3.15	A3 (0.25)	3.15
A4 (8)	3.50	3.20	3.28	3.22	2.98	A4 (0.25)	2.98
A5 (18)	3.05	2.82	3.17	3.00	2.69	A5 (0.25)	2.69
A6 (36)	2.43	2.48	2.86	2.86	2.65	A6 (0.05)	2.43
A7 (72)	1.81	2.05	2.46	2.48	2.36	A7 (0.10)	2.05
A8 (108)	1.41	1.64	2.07	2.10	2.02	A8 (0.10)	1.64
A9 (144)	1.14	1.34	1.69	1.78	1.73	A9 (0.10)	1.34

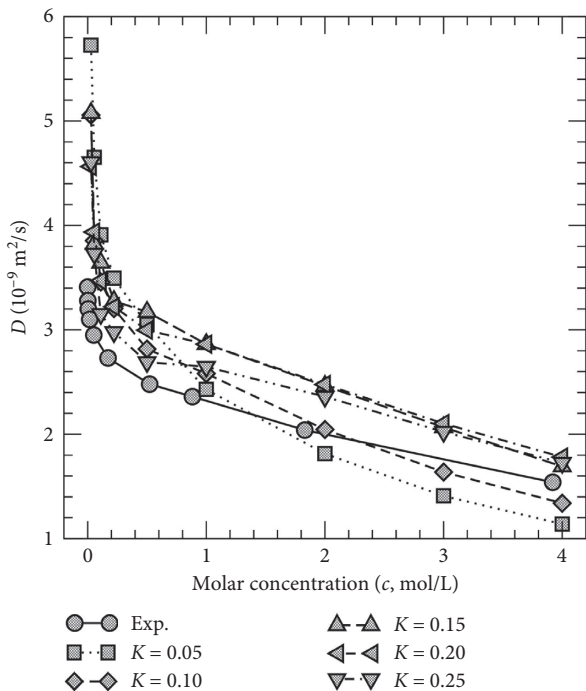


FIGURE 1: Comparison of the diffusion coefficients ($D = D_{\text{Na}^+} + D_{\text{Cl}^-}$) of NaCl at 25°C as a function of the molar concentration (c) of NaCl for given Ewald sum parameters (κ) employing a velocity Verlet algorithm obtained from MSDs of our MD simulations with the experimental data [23].

that the MD results D for all the Ewald sum parameter κ overestimate the experimental data (\circ) except those (\diamond) with $\kappa = 0.10 \text{ \AA}^{-1}$ at 3.0 and 4.0 mol/L and those (\square) with $\kappa = 0.05 \text{ \AA}^{-1}$ at 2.0, 3.0, and 4.0 mol/L.

When compared with the experimental data, the best MD results for D are obtained at 0.0278–0.50 mol/L with $\kappa = 0.25 \text{ \AA}^{-1}$ (∇), at 1.0 M with $\kappa = 0.05 \text{ \AA}^{-1}$ (\square), and at 2.0–4.0 mol/L with $\kappa = 0.10 \text{ \AA}^{-1}$ (\diamond). This best result set of D is also listed in Table 3. In our previous MD study [8], the Ewald sum parameter $\kappa = 0.20$ – 0.30 \AA^{-1} gives the best result for the ionic mobility μ_{Na^+} and μ_{Cl^-} at 25°C in single-ion systems in 1023 SPC/E water molecules. However, in the current work for multi-ion systems, the numbers of SPC/E water molecules are in the range of $N_w = 1800$ – 2000 . Note that the best results of D for $N_{\text{NaCl}} = 1, 2, 4, 8$, and 18 (the

A1 ~ A5 MD systems) are obtained with $\kappa = 0.25 \text{ \AA}^{-1}$ which also gives the best result for μ_{Na^+} and μ_{Cl^-} in single-ion systems in 1023 SPC/E water molecules. [2].

In Figure 2, we have compared the best obtained D (\square) and D with $\kappa = 0.10 \text{ \AA}^{-1}$ (\diamond) as a function of c with the experimental data (\circ). However, the obtained structural and dynamic properties of the MD systems are totally different for the different values of the Ewald sum parameter κ , which is discussed in the following sections. Instead of choosing the MD systems for the best obtained D to the experimental data with different κ , we have chosen those of the same $\kappa = 0.10 \text{ \AA}^{-1}$ which give D (\diamond) closest to the experimental data among those with the same κ , but less closer to the best obtained D with different κ . Figure 2 also shows D_{Na^+} and D_{Cl^-} with $\kappa = 0.10 \text{ \AA}^{-1}$ as a function of c . D_{Cl^-} at all the c (mol/L) is greater than D_{Na^+} , and these two values become equal as c increases.

At very low concentrations, the D values of NaCl are much higher than the experimental data, the values at 0.222 and 0.5 mol/L are slightly higher than the experimental data, and the values at 1.0 and 2.0 mol/L are similar to the experimental data. At 3.0 and 4.0 mol/L, it is slightly lower than the experimental data. This result can be highly dependent on the choice of the Ewald sum parameter, κ , as discussed above.

3.2. Molar Conductivity. We plotted molecular conductivity $\Lambda_m (= \lambda_{\text{Na}^+} + \lambda_{\text{Cl}^-})$ of NaCl as a function of $c^{1/2}$ obtained from D in our MD simulations in the inset of Figure 2, where $\lambda_i = D_i z_i^2 F^2 / RT$, where z_i is the charge on the ion in units of the electronic charge e , F is the Faraday constant, R is the gas constant, and T is the absolute temperature.

Both the experimental data and the MD results for Λ_m of NaCl show two linear dependences (Ex1 and Ex2) as a function of $c^{1/2}$. The value of the first slope for the first 4 experimental points (Exp. Ex1) and that of the second slope for the rest 6 points (Exp. Ex2) are -8.83 and $-2.94 \text{ mS m}^2 \text{ mol}^{-1} / (\text{mol} \cdot \text{L}^{-1})^{1/2}$, respectively. Those for the first 3 MD results (MD Ex1) and the rest 6 results (MD Ex2) are -34.73 and $-4.47 \text{ mS m}^2 \text{ mol}^{-1} / (\text{mol} \cdot \text{L}^{-1})^{1/2}$, respectively. According to the Debye–Hückel–Onsager (DHO) theory, equation (3), the slope ($A + B \Lambda_m^o$) is equal to $-8.91 \text{ mS m}^2 \text{ mol}^{-1} / (\text{mol} \cdot \text{L}^{-1})^{1/2}$ with the numerical values of A and B in water, $6.02 \text{ mS m}^2 \text{ mol}^{-1} / (\text{mol} \cdot \text{L}^{-1})^{1/2}$ and $0.229 \text{ (mol} \cdot \text{L}^{-1})^{1/2}$, and Λ_m^o of NaCl, $12.64 \text{ mS m}^2 \text{ mol}^{-1}$ [1]. In

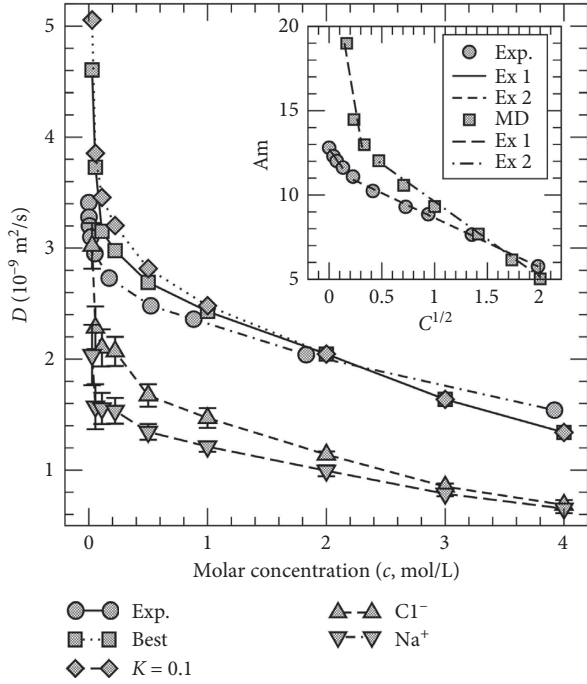


FIGURE 2: Comparison of the best diffusion coefficients (D), those with $\kappa = 0.10 \text{ \AA}^{-1}$, and D_{Na^+} and D_{Cl^-} at 25°C as a function of c with the experimental data [23]. The inset shows comparison of molar conductivity (Λ_m) of NaCl as a function of $c^{1/2}$ obtained from D with the experimental data.

conclusion, the MD results for Λ_m of NaCl show two linear dependences like the experimental result, but the value of the first slope is too large for the DHO theory and the value of the second slope is similar to the experimental result.

3.3. Radial Distribution Functions $g_{iw}(r)$ and Running Hydration Numbers $n_{iw}(r)$. The radial distribution functions, $g_{io}(r)$ and $g_{ih}(r)$, and the running hydration numbers, $n_{io}(r)$, for the ions (Na^+ or Cl^-) and the O or H atoms of SPC/E water molecules are shown in Figure 3 for the A6 MD system ($c = 1.0 \text{ mol/L}$, each $Na^+(Cl^-)$ 36 ions with 1956 water molecules) with $\kappa = 0.10 \text{ \AA}^{-1}$ as a function of distance. The running hydration number is defined as

$$n_{ij}(r) = \int_0^r g_{ij}(r') 4\pi r'^2 dr'. \quad (11)$$

Figure 3 shows the typical $g_{iw}(r)$ functions with positions of $g_{ClO}(r)$ at the first maximum 3.25 \AA and the first minimum 3.95 \AA , of $g_{Cl-H}(r)$ at the first maximum 2.30 \AA and the first minimum 3.10 \AA , $g_{NaO}(r)$ at the first maximum 2.35 \AA and the first minimum 3.15 \AA and $g_{NaH}(r)$ at the first maximum 3.00 \AA and the first minimum 3.75 \AA . The positions of the first maxima and minima of $g_{io}(r)$ and $g_{ih}(r)$ are almost the same for all the values of c and κ considered in this study and the magnitudes of those maxima and minima are very slightly different for all c and κ . These radial distribution functions $g_{iw}(r)$ of multi-ion systems are almost the same to those of single-ion systems [2].

The hydration number $n_{io}(R_1)$ in the first shell is defined through equation (11) from the ion-oxygen distribution functions $g_{io}(r)$ where the upper limit of integration R_1 is the radius of the first hydration sphere, which corresponds to the first minimum in $g_{io}(r)$. That is, $R_1 = 3.95 \text{ \AA}$ for $g_{ClO}(r)$ and 3.15 \AA for $g_{NaO}(r)$. We have listed the average hydration numbers $n_{NaO}(R_1)$ and $n_{ClO}(R_1)$ for the values of $\kappa = 0.05, 0.10$ and 0.25 \AA^{-1} in the first hydration shells of Na^+ and Cl^- in SPC/E water at 25°C in Table 4. The values of $n_{NaO}(R_1)$ and $n_{ClO}(R_1)$ are almost the same for $\kappa = 0.05 \text{ \AA}^{-1}$ (5.64–5.85 and 7.55–7.62), $\kappa = 0.10 \text{ \AA}^{-1}$ (5.67–5.90 and 7.65–7.82), and $\kappa = 0.25 \text{ \AA}^{-1}$ (5.47–5.69 and 7.51–7.68).

3.4. Radial Distribution Functions $g_{ii}(r)$ and Running Coordination Numbers $n_{ii}(r)$. The MD systems of small numbers of ion(s) – the A1 [each $Na^+(Cl^-)$ 1 ion] and the A2 [each $Na^+(Cl^-)$ 2 ions] show unstructured $g_{ii}(r)$ functions due to the very small numbers of ion(s). The radial distribution functions, $g_{NaNa}(r)$, $g_{NaCl}(r)$, and $g_{ClCl}(r)$, and the running coordination numbers, $n_{NaNa}(r)$, $n_{NaCl}(r)$, and $n_{ClCl}(r)$ at 25°C for the A6 MD system [$c = 1.0 \text{ mol/L}$, each $Na^+(Cl^-)$ 36 ions with 1956 water molecules] with $\kappa = 0.25 \text{ \AA}^{-1}$ and $\kappa = 0.10 \text{ \AA}^{-1}$ are shown in Figures 4 and 5, respectively. The radial distribution functions $g_{ii}(r)$ of other MD systems (the A3 ~ A5 and the A7 ~ A9) with the same $\kappa = 0.25 \text{ \AA}^{-1}$ are very similar to those of the A6 (Figure 4) with slightly different magnitudes of peaks, which are rather similar to the ordinary $g_{iw}(r)$ functions (Figure 3). However, the $g_{ii}(r)$ functions with different κ are totally different. For comparison, we show the $g_{ii}(r)$ and $n_{ii}(r)$ functions of the A6 MD system with $\kappa = 0.10 \text{ \AA}^{-1}$ in Figure 5, in which a dramatic change occurs with a very deep minimum of $g_{NaCl}(r)$ and, as a result, sharp maxima of $g_{NaNa}(r)$ and $g_{ClCl}(r)$ at the distance 9.95 \AA . Which is closer to nature, $\kappa = 0.10 \text{ \AA}^{-1}$ or 0.25 \AA^{-1} ?

Other MD systems (the A3 ~ A5 and the A7 ~ A9) with the same $\kappa = 0.10 \text{ \AA}^{-1}$ have also almost the same $g_{ii}(r)$ to those of the A6 (Figure 5) with slightly different magnitudes of peaks. Also, the $g_{ii}(r)$ functions for the A3 ~ A9 MD systems with $\kappa = 0.0$ (no Ewald sum), 0.05 \AA^{-1} , and 0.15 \AA^{-1} are similar to those for those MD system with $\kappa = 0.10 \text{ \AA}^{-1}$ (Figure 5), but the running coordination numbers $n_{ii}(r)$ are different, while those $g_{ii}(r)$ for the A3 ~ A9 MD systems with $\kappa = 0.20 \text{ \AA}^{-1}$ are similar to those with $\kappa = 0.25 \text{ \AA}^{-1}$ (Figure 4). In Figure 5, $g_{NaNa}(r)$ and $g_{ClCl}(r)$ at short distances are nonzero but the corresponding average $n_{NaNa}(r)$ at 5.0 \AA and $n_{ClCl}(r)$ at 6.5 \AA are very small, 0.17 and 0.21, respectively, but $n_{NaCl}(r)$ at 5.0 \AA and 6.5 \AA are already 0.28 and 1.20. As the distance r increases, $n_{NaNa}(r)$ and $n_{ClCl}(r)$ increase slowly, then suddenly reaching 2.04 and 2.10 at 9.95 \AA , while the corresponding average $n_{NaCl}(r)$ is 2.73 at 8.0 \AA and slowly reaches about 3.80 at 9.95 \AA .

3.5. Ionic Atmosphere. We have also listed the average coordination numbers $n_{NaNa}(R_1)$, $n_{ClCl}(R_1)$, and $n_{NaCl}(R_1)$ ($= n_{ClNa}(R_1)$) for the A3 ~ A9 MD systems with $\kappa = 0.10 \text{ \AA}^{-1}$ in the coordination shells around Na^+ and Cl^- at 25°C with $R_1 = 9.95 \text{ \AA}$ in Table 5, while the coordination numbers n_{ii}

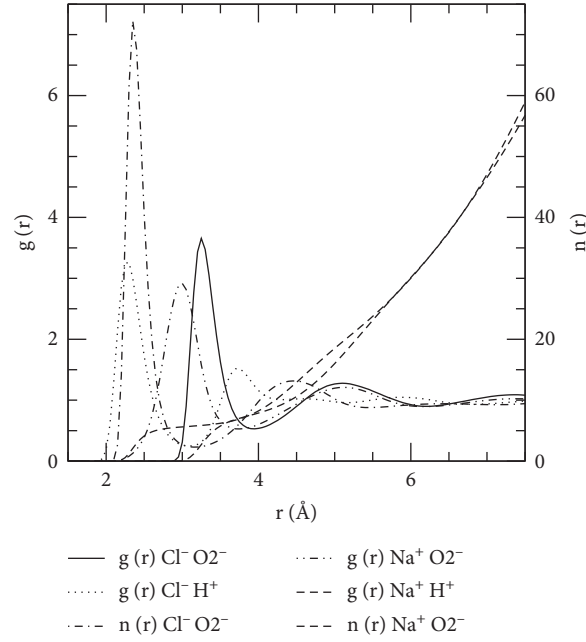


FIGURE 3: Radial distribution functions $g_{io}(r)$ and $g_{ih}(r)$ and the running hydration numbers $n_{io}(r)$ and $n_{ih}(r)$ of SPC/E water molecules for the A6 MD system at 25°C as a function of the distance r (Å) between the ion (i) and the oxygen (O) and hydrogen atom (H) of a water molecule using Ewald sum with $\kappa=0.10 \text{ Å}^{-1}$.

TABLE 4: The average hydration numbers ($n_{io}(R_1)$) and residence times (τ_{io} , ps) of water molecules in the first hydration shells of Na^+ and Cl^- in SPC/E water at 25°C employing a velocity Verlet algorithm where $R_1 = 3.15 \text{ Å}$ for Na^+ and $R_1 = 3.95 \text{ Å}$ for Cl^- .

System	$\kappa = 0.05 \text{ Å}^{-1}$				$\kappa = 0.10 \text{ Å}^{-1}$				$\kappa = 0.25 \text{ Å}^{-1}$			
	$n_{\text{NaO}}(R_1)$	τ_{NaO}	$n_{\text{ClO}}(R_1)$	τ_{ClO}	$n_{\text{NaO}}(R_1)$	τ_{NaO}	$n_{\text{ClO}}(R_1)$	τ_{ClO}	$n_{\text{NaO}}(R_1)$	τ_{NaO}	$n_{\text{ClO}}(R_1)$	τ_{ClO}
A1	5.65	12.9	7.62	8.59	5.67	13.5	7.82	9.26	5.69	14.0	7.58	9.26
A2	5.66	15.6	7.63	9.52	5.70	18.0	7.82	9.86	5.65	18.6	7.64	10.4
A3	5.66	16.7	7.63	9.38	5.71	18.7	7.82	10.3	5.68	19.4	7.51	12.0
A4	5.66	16.3	7.59	9.56	5.70	18.2	7.81	10.6	5.69	21.3	7.52	12.1
A5	5.64	14.3	7.57	9.43	5.70	18.4	7.78	10.5	5.67	21.2	7.54	12.8
A6	5.67	13.8	7.55	9.47	5.74	18.0	7.78	11.1	5.64	22.4	7.59	13.1
A7	5.78	13.2	7.59	9.75	5.76	17.9	7.65	11.7	5.53	23.7	7.63	14.2
A8	5.85	14.0	7.62	10.3	5.90	18.8	7.69	12.6	5.47	25.8	7.68	15.6
A9	5.94	13.9	7.65	10.8	5.98	20.0	7.72	14.1	5.31	28.0	7.71	17.1

(R_1) for the A3 ~ A9 MD systems with $\kappa=0.25 \text{ Å}^{-1}$ are not defined since $g_{ii}(r)$ for $\kappa=0.25 \text{ Å}^{-1}$ show neither any clear maxima for $g_{\text{ClCl}}(r)$ and $g_{\text{NaNa}}(r)$ at $R_1 = 9.95 \text{ Å}$ nor a clear minimum for $g_{\text{NaCl}}(r)$ at $R_1 = 9.95 \text{ Å}$. For the A3 (each $\text{Na}^+(\text{Cl}^-)$ 4 ions) and the A4 (each $\text{Na}^+(\text{Cl}^-)$ 8 ions), $n_{\text{NaNa}}(R_1)$ and $n_{\text{ClCl}}(R_1)$ are less than 1. The ratios of $n_{\text{NaCl}}(R_1)/(n_{\text{NaNa}}(R_1)+1)$ and $n_{\text{ClNa}}(R_1)/(n_{\text{ClCl}}(R_1)+1)$ for the A5 ~ A9 MD systems are greater than 1 which indicates a characteristic of ionic atmosphere: Averaged over time, counterions are more likely to be found by any given ion. The time averaged, spherical haze, in which counterions outnumber ions of the same charge as the central ion, has a net charge opposite in sign to that on the central ion.

Relating to the running coordination numbers, $n_{\text{NaNa}}(r)$, $n_{\text{NaCl}}(r)$, and $n_{\text{ClCl}}(r)$ as seen in Table 5, we can imagine an imaginary sphere with Na^+ at the origin and 9.95 Å from it, filled with water molecules, with more number of Cl^- inside the sphere and less number of Na^+ near the surface of the

sphere. Figure 6 shows a snapshot of the ionic atmosphere with Na^+ at the origin and 9.95 Å from it, obtained from our MD simulation. Since an electric field is not applied to a solution of ions in this study, an asymmetric ionic atmosphere, the relaxation and the electrophoretic effects are not observed, but it is currently under studying by applying an electric field to a solution of ion.

3.6. Residence Time Correlation Functions and Residence times. The residence times are calculated from time correlation functions [8–10, 24] defined by

$$R(r, t) = \frac{1}{N_h} \sum_{i=1}^{N_h} [\theta_i(r, 0) \cdot \theta_i(r, t)], \quad (12)$$

where $\theta_i(r, t)$ is the Heaviside unit step function, which is 1 if a water molecule i is in a region r within the coordination

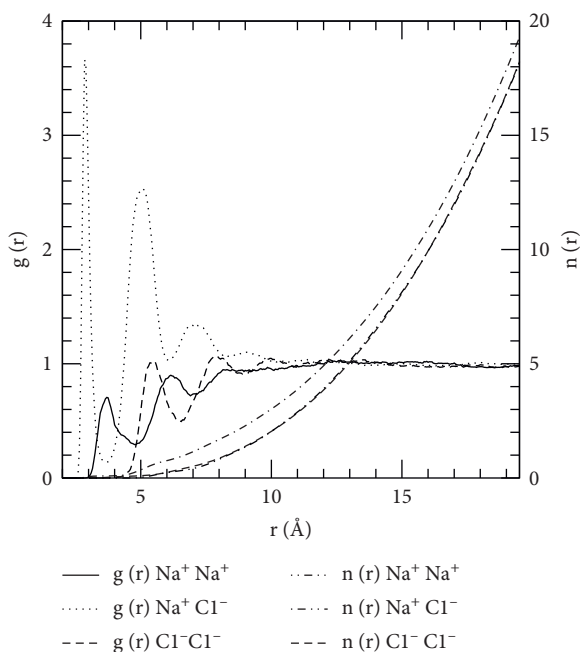


FIGURE 4: Radial distribution functions $g_{\text{NaNa}}(r)$, $g_{\text{NaCl}}(r)$, and $g_{\text{ClCl}}(r)$, and the running coordination numbers, $n_{\text{NaNa}}(r)$, $n_{\text{NaCl}}(r)$, and $n_{\text{ClCl}}(r)$ for the A6 MD system at 25°C as a function of r (Å) between the ions (i) using Ewald sum with $\kappa = 0.25 \text{ Å}^{-1}$.

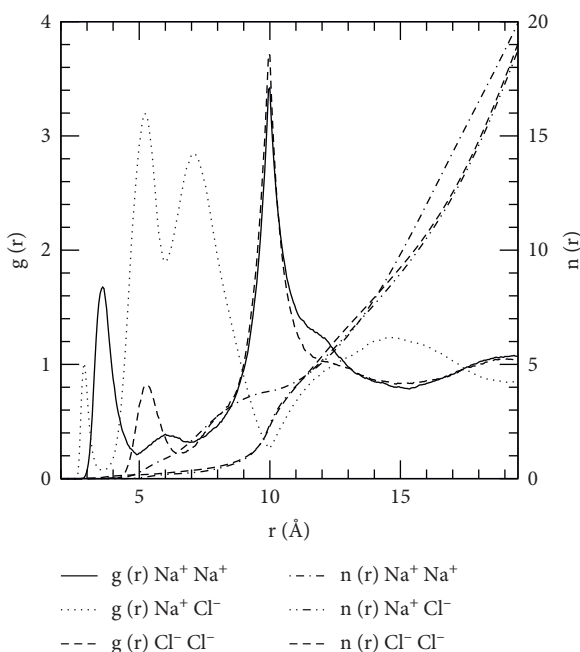


FIGURE 5: Radial distribution functions $g_{\text{NaNa}}(r)$, $g_{\text{NaCl}}(r)$, and $g_{\text{ClCl}}(r)$, and the running coordination numbers, $n_{\text{NaNa}}(r)$, $n_{\text{NaCl}}(r)$, and $n_{\text{ClCl}}(r)$ for the A6 MD system at 25°C as a function of r (Å) between the ions (i) using Ewald sum with $\kappa = 0.10 \text{ Å}^{-1}$.

shell around the ion at time t and 0 otherwise, and N_h is the average number of water molecules in this region r at $t=0$ [8–10, 24]. Figure 7 shows the time dependence of $\ln[R(r, t)]$ for water in the first hydration shell of the Na^+ and Cl^-

ions with $R_1 = 3.95 \text{ Å}$ for $g_{\text{ClO}}(r)$ and 3.15 Å for $g_{\text{NaO}}(r)$ and that for Na^+ or Cl^- in the coordination shell around the Cl^- or Na^+ with $R_1 = 9.95 \text{ Å}$ at 25°C calculated from our MD simulations. The residence time t is obtained by fitting the time correlation function to an exponential decay $\langle R(r, t) \rangle > \exp(-t/\tau)$, which is useful particularly when t is large. Table 4 shows the average residence times of water in the first hydration shell of the Na^+ and Cl^- ions for all the MD systems with $\kappa = 0.05 \text{ Å}^{-1}$, 0.10 Å^{-1} , and 0.25 Å^{-1} .

In Table 4, the values of τ_{NaO} and τ_{ClO} for the A1 MD system are exceptionally smaller than those for the other MD systems. τ_{NaO} are always greater than τ_{ClO} with given values of κ and both the residence times increase with κ for all the systems. Roughly saying, τ_{NaO} with $\kappa = 0.05 \text{ Å}^{-1}$ increases and decreases with the concentration of NaCl, c , and τ_{ClO} increases monotonically with c , while τ_{NaO} and τ_{ClO} with $\kappa = 0.10$ and 0.25 Å^{-1} increase with c . Generally, both residence times for all the MD systems with $\kappa = 0.05 \text{ Å}^{-1}$ are too low, those with $\kappa = 0.25 \text{ Å}^{-1}$ are too high, and those with $\kappa = 0.10 \text{ Å}^{-1}$ are moderate.

Table 5 shows the average residence times of Na^+ and Cl^- in the coordination shell around Na^+ and Cl^- with $R_1 = 9.95 \text{ Å}$ for the A3 ~ A9 systems with $\kappa = 0.10 \text{ Å}^{-1}$. Approximately, the values of τ_{NaNa} and τ_{ClCl} are in the range of 20–50 ps, while τ_{NaCl} and τ_{ClNa} are in that of 110 and 115 ps. Also, τ_{NaNa} and τ_{ClCl} increase with c , while τ_{NaCl} and τ_{ClNa} are independent of c . The ratios of $\tau_{\text{NaCl}}/\tau_{\text{NaNa}}$ and $\tau_{\text{ClNa}}/\tau_{\text{ClCl}}$ for the A5 ~ A9 MD systems are greater than 1 which indicates that oppositely charged ions attract each other. Also, the increase of τ_{NaNa} and τ_{ClCl} and, as a result, the decrease of the ratios of $\tau_{\text{NaCl}}/\tau_{\text{NaNa}}$ and $\tau_{\text{ClNa}}/\tau_{\text{ClCl}}$ with c means that the migration of Na^+ (or Cl^-) occurs hardly due to the increasing numbers of Na^+ (or Cl^-)

3.7. Water Diffusion. We have listed diffusion coefficients D_w of SPC/E water at 25°C for the all MD systems with $\kappa = 0.05$, 0.10 , and 0.25 Å^{-1} in Table 6. For the pure water system, a recent MD simulation study [25] of 1024 SPC/E water molecules using Ewald with $\kappa = 0.20 \text{ Å}^{-1}$ employing the vV algorithm reported $2.78 \times 10^{-9} \text{ m}^2/\text{s}$ obtained from MSD (mean square displacement, equation (9)) and $2.75 \times 10^{-9} \text{ m}^2/\text{s}$ from VAC (velocity autocorrelation, equation (10)) function at 300 K, which overestimate the experimental data at the same temperature ($2.39 \times 10^{-9} \text{ m}^2/\text{s}$ [26, 27] and $2.49 \times 10^{-9} \text{ m}^2/\text{s}$ [26–28]). However, TIP4P/2005 water model [29] gives an excellent agreement, $2.39 \times 10^{-9} \text{ m}^2/\text{s}$, obtained from both the MSD and VAC in our previous study [25] with the experiment one.

D_w obtained from our recent MD simulations [8] as a function of RFC (reaction field correction), ST (simple truncation), and Ewald sum parameter employing the Gear algorithm overestimates the experimental data, while D_w employing the vV algorithm underestimates except for ST and Ewald with $\kappa > 0.45 \text{ Å}^{-1}$. These MD simulations [8] reported that D_w is $3.03 \times 10^{-9} \text{ m}^2/\text{s}$ in the Na^+ -water system and $3.09 \times 10^{-9} \text{ m}^2/\text{s}$ in the Cl^- -water system using ST employing the Gear algorithm with $N_w = 215$ of SPC/E water. An MD simulation for alkali Earth metal cations (Mg^{2+} ,

TABLE 5: Average coordination numbers ($n_{ij}(R_1)$) and residence times (τ_{ij} , ps) of Na^+ and Cl^- in the first coordination shells around Na^+ and Cl^- in SPC/E water at 25°C with $\kappa = 0.10 \text{ \AA}^{-1}$ employing a velocity Verlet algorithm where $R_1 = 9.95 \text{ \AA}$. $n_{ij}(R_1)^* = n_{ij}(R_1) + 1$.

System	$n_{\text{NaNa}}(R_1)$	τ_{NaNa}	$n_{\text{ClCl}}(R_1)$	τ_{ClCl}	$n_{\text{NaCl}}(R_1)$	τ_{NaCl}	$n_{\text{ClNa}}(R_1)$	τ_{ClNa}	$n_{\text{NaCl}}(R_1)/n_{\text{NaNa}}(R_1)^*$	$n_{\text{ClNa}}(R_1)/n_{\text{ClCl}}(R_1)^*$	$\tau_{\text{NaCl}}/\tau_{\text{NaNa}}$	$\tau_{\text{ClNa}}/\tau_{\text{ClCl}}$
A3	.118	12.8	.182	14.6	.632	55.3	.632	58.0	—	—	4.32	3.97
A4	.371	15.2	.374	17.6	1.22	74.5	1.22	94.0	—	—	4.90	5.34
A5	1.25	22.1	1.41	25.0	2.70	110.	2.70	120.	1.20	1.12	4.98	4.80
A6	2.04	27.0	2.10	29.6	3.80	115.	3.80	114.	1.25	1.23	4.26	3.85
A7	3.67	34.3	3.95	38.1	5.84	102.	5.84	102.	1.25	1.18	2.97	2.68
A8	5.83	42.2	6.33	48.2	8.29	106.	8.29	108.	1.21	1.13	2.51	2.24
A9	7.93	48.6	8.55	51.3	10.7	115.	10.7	115.	1.20	1.12	2.37	2.24

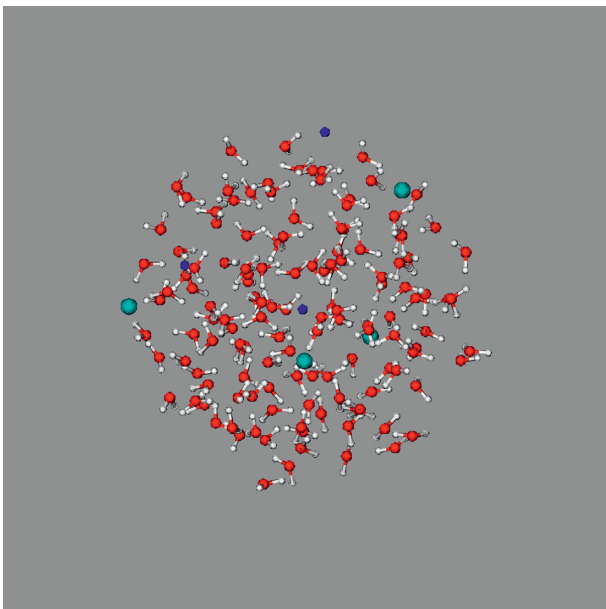


FIGURE 6: A snapshot of ionic atmosphere with Na^+ at the origin and $R_1 = 9.95 \text{ \AA}$ from it, filled with 132 water molecules at 25°C. 3 Na^+ : dark blue and 4 Cl^- : dark cyan.

Ca^{2+} , Sr^{2+} , and Ba^{2+}) in an aqueous solution at 25°C of SPC/E water potential ($N_w = 215$) using Ewald employing the Gear algorithm reported that D_w is in the range of $2.46\text{--}2.62 \times 10^{-9} \text{ m}^2/\text{s}$ [17].

In Table 6, roughly speaking, D_w with $\kappa = 0.05 \text{ \AA}^{-1}$ increases up to the A7 MD system with slow decreases as c increases, while D_w with $\kappa = 0.10 \text{ \AA}^{-1}$ has almost the same values up to the A6 MD system with sudden decreases, and D_w with $\kappa = 0.25 \text{ \AA}^{-1}$ decreases monotonically up to the A6 MD system with sudden decreases. The behavior of D_w with $\kappa = 0.10 \text{ \AA}^{-1}$ seems to be the most reasonable one: D_w has almost the same values up to $n = 36$ $\text{Na}^+(\text{Cl}^-)$ ions and decreases suddenly for $n = 72$, 108, and 144.

In a study of the system-size dependence of translational diffusion coefficients and viscosities of pure water in molecular dynamics simulations under periodic boundary conditions [30], for a cubic simulation box of length L , the diffusion coefficient is corrected for system-size effects as $D_0 = D_{\text{PBC}} + 2.837297 k_B T / (6\pi\eta L)$, where D_{PBC} is the diffusion coefficient calculated in the simulation, k_B is the Boltzmann constant, T is the absolute temperature, and η is

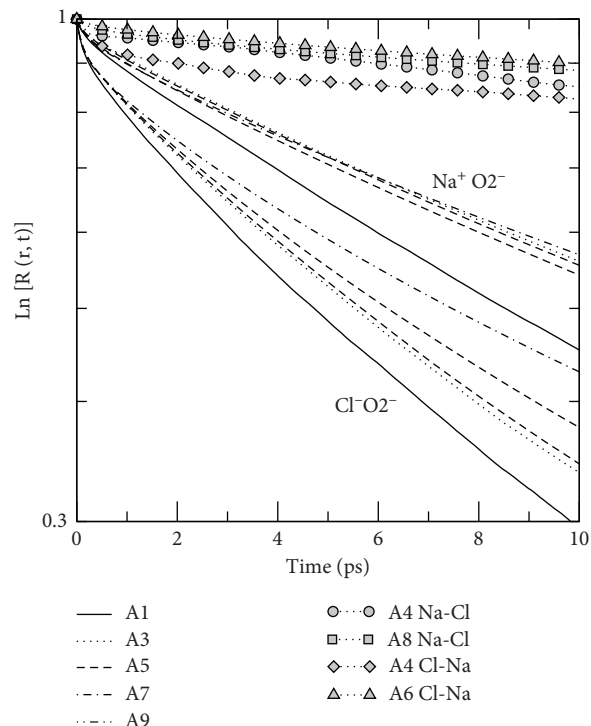


FIGURE 7: Logarithm of residence time correlation functions for the hydrated SPC/E water molecules at 25°C in the first hydration shell of Na^+ and Cl^- and that for Na^+ or Cl^- in the coordination shell around Cl^- or Na^+ with $R_1 = 9.95 \text{ \AA}$ obtained from our MD simulations with $\kappa = 0.10 \text{ \AA}^{-1}$.

the shear viscosity of the solvent. Using $T = 298.15 \text{ K}$ and $L = 39.1009 \text{ \AA}$ for our systems and $\eta = 0.854 \text{ cP}$ at 300 K, $D_0 - D_{\text{PBC}} = 0.1856 \times 10^{-9} \text{ m}^2/\text{s}$ which is quite small, compared to our calculated $D_w = 2.02\text{--}2.84 \times 10^{-9} \text{ m}^2/\text{s}$ with $\kappa = 0.10 \text{ \AA}^{-1}$ (Table 6). This correction for D_w is not included in this study.

A recent study [31] reported that the effect of salt on the dynamics of water molecules follows the Hofmeister series. For some structure-making salts, the self-diffusion coefficient of the water molecules, D_w , decreases with increasing salt concentration and for other structure-breaking salts, D_w increases with increasing salt concentration c . Both ratios of experimental and simulation $D_w(\text{NaCl})/D_0(\text{bulk})$ almost linearly decrease with c up to 0.75 and 0.5 at $c = 4 \text{ M}$.

A more recent study [32] reported that when used with a good-quality water model, e.g., TIP4P/2005 [29] or E3B [33],

TABLE 6: Water diffusion coefficients ($10^{-9} \text{ m}^2/\text{s}$) at 25°C employing a velocity Verlet algorithm, where n is the number of ($\text{Na}^+ + \text{Cl}^-$) ions.

System (n)	$\kappa = 0.05 \text{ \AA}^{-1}$	$\kappa = 0.10 \text{ \AA}^{-1}$	$\kappa = 0.25 \text{ \AA}^{-1}$
A1 (2)	2.74	2.81	2.68
A2 (4)	2.76	2.79	2.66
A3 (8)	2.80	2.82	2.64
A4 (16)	2.87	2.82	2.62
A5 (36)	3.01	2.84	2.52
A6 (72)	3.15	2.80	2.38
A7 (144)	3.25	2.58	2.05
A8 (216)	3.14	2.32	1.76
A9 (288)	2.94	2.02	1.51

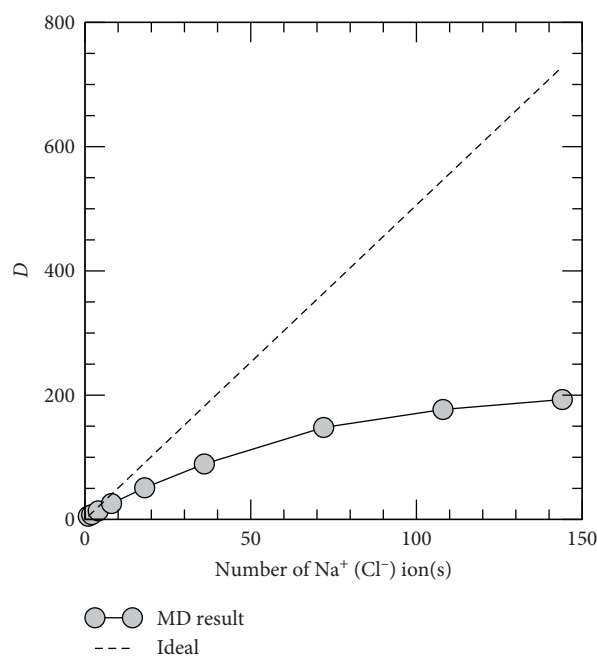
this method recovers the qualitative behavior of the water diffusion trends of experiment shown that the water diffusion coefficient increases in the presence of salts of low charge density (e.g., CsI), whereas the results of simulations with nonpolarizable models show a decrease of the water diffusion coefficient in all alkali halide solutions.

3.8. Energetics. Equations (7) and (8) have 18 potential energies, which are (1) water-water, (2) water- Na^+ , (3) water- Cl^- , (4) Na^+ - Na^+ , (5) Cl^- - Cl^- , and (6) Na^+ - Cl^- LJ potential energy and the corresponding electrostatic (Coulomb) energy in real and reciprocal spaces for the Ewald sum. The important potential energy that determines the molar conductivity of an electrolyte can be the electrostatic energy of ion-ion in real space and reciprocal spaces for the Ewald sum. In Table 7, we compared the average electrostatic energies of the electrolytic system obtained using the Ewald sum of $\kappa = 0.10 \text{ \AA}^{-1}$ and the velocity Verlet algorithm. Na^+ - Na^+ and Cl^- - Cl^- electrostatic energies in real space increase monotonically as the number of Na^+ (Cl^-) ions increases and the corresponding Na^+ - Cl^- energy also increases negatively, whereas the corresponding electrostatic energies in reciprocal space increase and decrease with the number of Na^+ (Cl^-) ions. The ion-ion electrostatic energy in real space seems to be more important than in reciprocal space when determining the molar conductivity of an electrolyte. Ion-ion electrostatic energy, which increases monotonically in real space with the number of Na^+ (Cl^-) ions, positively or negatively, retards the diffusion of ions. In conclusion, the molar conductivity of the electrolyte decreases with the concentration of the electrolyte.

The molar conductivity of an electrolyte is found to vary with the concentration. One reason for this variation is that the number of ions in the solution might not be proportional to the concentration of the electrolyte (that is, a strong or a weak electrolyte). Second, because ions interact with each other strongly, the conductivity of a solution is not exactly proportional to the number of ions present. Figure 8 shows the sum of diffusion coefficients (\circ) of all ions multiplied by n in D_{A1} to D_{A9} in Table 3 for systems A1 to A9 for $\kappa = 0.10 \text{ \AA}^{-1}$. The sum of the “Ideal” diffusion coefficients (---) of all ions obtained from D_{A1} multiplied by n in Table 3 for all identical systems is also shown. Here, of course, the molar conductivity of a solution is exactly proportional to the number of ions

TABLE 7: The average electrostatic energies (kJ/mol) per ion of the electrolyte systems using Ewald sum with $\kappa = 0.10 \text{ \AA}^{-1}$ employing a velocity Verlet algorithm, where n is the number of (Na^+ or Cl^-) ion(s).

System (n)	Na^+ - Na^+		Cl^- - Cl^-		Na^+ - Cl^-	
	Real	reciprocal	Real	reciprocal	Real	reciprocal
A1 (1)	—	—	—	—	-0.29	3.83
A2 (2)	0.00	13.4	0.93	15.7	-11.0	-2.16
A3 (4)	1.70	30.9	2.89	26.5	-23.3	-7.59
A4 (8)	6.86	33.2	6.67	34.9	-48.2	-18.0
A5 (18)	34.1	38.0	29.9	39.3	-100	-42.8
A6 (36)	52.8	34.5	42.7	31.7	-131	-32.9
A7 (72)	107	15.9	90.2	14.1	-193	-13.5
A8 (108)	182	14.4	162	12.8	-272	-11.9
A9 (144)	257	4.91	232	4.61	-347	-4.05

FIGURE 8: Sum of diffusion coefficients of all the ions in the systems. MD result: multiplied by n in D_{A1} to D_{A9} in Table 3 for systems A1 to A9 for $\kappa = 0.10 \text{ \AA}^{-1}$ and ideal: obtained from D_{A1} multiplied by n in Table 3 for all identical systems.

present. The deviation of the sum (○) of the diffusion coefficients from the “Ideal” diffusion coefficient (---) is due to the delay of the moving ions due to the strong ion-ion electrostatic interaction in real space as described above.

4. Conclusions

We have carried out molecular dynamics (MD) simulations of NaCl in SPC/E water at 25°C to calculate the molar conductivity Λ_m of NaCl as a function of NaCl concentration (c) using Ewald sums employing a velocity Verlet algorithm.

It is found that the structural properties of the MD systems with different κ are totally different. The obtained ion-ion radial distribution functions $g_{ii}(r)$ with $\kappa = 0.25 \text{ \AA}^{-1}$ show the ordinary behavior similar to the ion-water radial distribution functions $g_{iw}(r)$. However, those functions $g_{ii}(r)$ with $\kappa = 0.10 \text{ \AA}^{-1}$ give a dramatic change with a very deep minimum of $g_{NaCl}(r)$ and, as a result, sharp maxima of $g_{NaNa}(r)$ and $g_{ClCl}(r)$ at the distance $R_1 = 9.95 \text{ \AA}$. The ratios of $n_{NaCl}(R_1)/(n_{NaNa}(R_1) + 1)$ and $n_{ClNa}(R_1)/(n_{ClCl}(R_1) + 1)$ for the A5 ~ A9 MD systems with $\kappa = 0.10 \text{ \AA}^{-1}$ are greater than 1 which indicates a characteristic of ionic atmosphere. This is the actual evidence of the basis of the Debye–Hückel theory of ionic solutions.

It is also found that the MD result for Λ_m of NaCl with Ewald sum parameter $\kappa = 0.10 \text{ \AA}^{-1}$ gives the closest one to the experimental data. The behavior of Λ_m is close to the experimental data except at very low concentrations which are much higher than the experimental data. The analysis of radial distribution functions, hydration numbers, coordination numbers around Na^+ and Cl^- , residence times of water around Na^+ and Cl^- , water diffusion, and ion-ion electrostatic energies support this finding. It has been found that the ion-ion electrostatic energy in real space plays an important role in explaining that the molar conductivity of the electrolyte decreases with concentration.

Compared with the experimental data, the best MD results of D_{Na^+} and D_{Cl^-} for $N_{\text{NaCl}} = 1, 2, 4, 8$, and 18 are obtained with $\kappa = 0.25 \text{ \AA}^{-1}$. This is consistent with the best result for μ_{Na^+} and μ_{Cl^-} in single-ion systems in 1023 SPC/E water molecules. [2] This indicates that the Ewald sum parameter $\kappa = 0.25 \text{ \AA}^{-1}$ is suitable for systems with a small number of ions and 1000 to 2000 water molecules. However, as the number of ions increases without significant fluctuations in the number of water molecules, κ changes for the best MD results of D_{Na^+} and D_{Cl^-} . We conclude that the appropriate value of κ is determined by the number of ions rather than the water molecule.

Data Availability

The data used in this study are given in the manuscript.

Conflicts of Interest

The author declares no conflicts of interest.

References

- [1] W. Atkins, *Physical Chemistry*, Oxford University Press, Oxford, USA, 5th edition, 1994.
- [2] M. Bester-Rogac, R. Neueder, and J. Barthel, “Conductivity of sodium chloride in water + 1,4-dioxane mixtures at temperatures from 5 to 35°C I. Dilute solutions,” *Journal of Solution Chemistry*, vol. 28, no. 9, pp. 1071–1086, 1999.
- [3] J. Barthel, H. Krienke, and W. Kunz, *Physical Chemistry of Electrolyte Solutions-Modern Aspects*, Steinkopff/ Darmstadt, and Springer, NY, USA, 1998.
- [4] M. Bester-Rogac, R. Neueder, and J. Barthel, “Conductivity of sodium chloride in water + 1,4-dioxane mixtures from 5 to 35°C. II. Concentrated solutions,” *Journal of Solution Chemistry*, vol. 29, no. 1, pp. 51–61, 2000.
- [5] O. Bernard, W. Kunz, P. Turq, and L. Blum, “Conductance in electrolyte solutions using the mean spherical approximation,” *The Journal of Physical Chemistry*, vol. 96, no. 9, pp. 3833–3840, 1992.
- [6] J. F. Casteel and E. S. Amis, “Specific conductance of concentrated solutions of magnesium salts in water-ethanol system,” *Journal of Chemical and Engineering Data*, vol. 17, no. 1, pp. 55–59, 1972.
- [7] J. Gujt, M. Bešter-Rogač, and B. Hribar-Lee, “An investigation of ion-pairing of alkali metal halides in aqueous solutions using the electrical conductivity and the Monte Carlo computer simulation methods,” *Journal of Molecular Liquids*, vol. 190, pp. 34–41, 2014.
- [8] S. H. Lee, “Ionic mobilities of Na^+ and Cl^- at 25°C as a function of Ewald sum parameter: a comparative molecular dynamics simulation study,” *Molecular Simulation*, vol. 46, no. 4, pp. 262–270, 2020.
- [9] S. H. Lee and J. C. Rasaiah, “Molecular dynamics simulation of ion mobility. 2. alkali metal and halide ions using the spc/e model for water at 25 °C,” *Journal of Physical Chemistry*, vol. 100, pp. 1420–1425, 1996.
- [10] H. J. C. Berendsen, J. R. Grigera, and T. P. Straatsma, “The missing term in effective pair potentials,” *The Journal of Physical Chemistry*, vol. 91, no. 24, pp. 6269–6271, 1987.
- [11] W. L. Jorgensen, “Revised TIP3 for simulations of liquid water and aqueous solutions,” *The Journal of Chemical Physics*, vol. 77, no. 8, pp. 4156–4163, 1982.
- [12] L. X. Dang, “Mechanism and thermodynamics of ion selectivity in aqueous solutions of 18-crown-6 ether: a molecular dynamics study,” *Journal of the American Chemical Society*, vol. 117, no. 26, pp. 6954–6960, 1995.
- [13] D. E. Smith and L. X. Dang, “Computer simulations of NaCl association in polarizable water,” *The Journal of Chemical Physics*, vol. 100, no. 5, pp. 3757–3766, 1994.
- [14] I. S. Joung and T. E. Cheatham, “Determination of alkali and halide monovalent ion parameters for use in explicitly solvated biomolecular simulations,” *The Journal of Physical Chemistry B*, vol. 112, no. 30, pp. 9020–9041, 2008.
- [15] F. Moucka, M. Lisal, M. J. Skvor, J. Jirak, I. Nezbeda, and W. R. Smith, “Molecular simulation of aqueous electrolyte solubility. 2. Osmotic ensemble monte carlo methodology for free energy and solubility calculations and application to NaCl,” *Journal of Physical Chemistry B*, vol. 115, pp. 7849–7861, 2011.
- [16] A. L. Benavides, M. A. Portillo, V. C. Chamorro, J. R. Espinosa, J. L. F. Abascal, and C. Vega, “A potential model for sodium chloride solution based on TIP4p/2005 water model,” *Journal of Chemical Physics*, vol. 147, no. 15, Article ID 104501, 2017.
- [17] S. H. Lee, “Molecular dynamics simulation study for ion mobility of alkali earth metal cations in water at 25°C,” *Molecular Simulation*, vol. 39, no. 11, pp. 895–901, 2013.

- [18] W. G. Hoover, A. J. C. Ladd, and B. Moran, "High-strain-rate plastic flow studied via nonequilibrium molecular dynamics," *Physical Review Letters*, vol. 48, no. 26, pp. 1818–1820, 1982.
- [19] D. J. Evans, "Computer "experiment" for nonlinear thermodynamics of Couette flow," *The Journal of Chemical Physics*, vol. 78, no. 6, pp. 3297–3302, 1983.
- [20] D. J. Evans, "On the representation of orientation space," *Molecular Physics*, vol. 34, no. 2, pp. 317–325, 1977.
- [21] D. J. Evans and S. Murad, "Singularity free algorithm for molecular dynamics simulation of rigid polyatomics," *Molecular Physics*, vol. 34, no. 2, pp. 327–331, 1977.
- [22] W. C. Swope, H. C. Andersen, P. H. Berens, and K. R. Wilson, "A computer simulation method for the calculation of equilibrium constants for the formation of physical clusters of molecules: application to small water clusters," *The Journal of Chemical Physics*, vol. 76, no. 1, pp. 637–649, 1982.
- [23] H. Hamann, A. Hamnett, and W. Vielstich, *Electrochemistry*, Wiley VCH, Berlin, Germany, 2nd edition, 2007.
- [24] R. W. Impey, P. A. Madden, and I. R. McDonald, "Hydration and mobility of ions in solution," *The Journal of Physical Chemistry*, vol. 87, no. 25, pp. 5071–5083, 1983.
- [25] S. H. Lee and J. Kim, "Transport properties of bulk water at 243–550 K: a Comparative molecular dynamics simulation study using SPC/E, TIP4P, and TIP4P/2005 water models," *Molecular Physics*, vol. 117, no. 14, pp. 1926–1933, 2019.
- [26] A. J. Easteal, W. E. Price, and L. A. Woolf, "Diaphragm cell for high-temperature diffusion measurements. Tracer Diffusion coefficients for water to 363 K," *Journal of the Chemical Society, Faraday Transactions 1: Physical Chemistry in Condensed Phases*, vol. 85, no. 5, pp. 1091–1097, 1989.
- [27] G. S. Kell, "Effects of isotopic composition, temperature, pressure, and dissolved gases on the density of liquid water," *Journal of Physical and Chemical Reference Data*, vol. 6, no. 4, pp. 1109–1131, 1977.
- [28] K. T. Gillen, D. C. Douglass, and M. J. R. Hoch, "Self-diffusion in liquid water to -31°C ," *The Journal of Chemical Physics*, vol. 57, no. 12, pp. 5117–5119, 1972.
- [29] J. L. F. Abascal and C. Vega, "A general purpose model for the condensed phase of water: TIP4P/2005," *Journal of Chemical Physics*, vol. 123, no. 12, Article ID 234505, 2005.
- [30] I.-C. Yeh and G. Hummer, "System-size dependence of diffusion coefficients and viscosities from molecular dynamics simulations with periodic boundary conditions," *The Journal of Physical Chemistry B*, vol. 108, no. 40, pp. 15873–15879, 2004.
- [31] J. S. Kim, Z. Wu, A. R. Morrow, A. Yethiraj, and A. Yethiraj, "Self-diffusion and viscosity in electrolyte solutions," *The Journal of Physical Chemistry B*, vol. 116, no. 39, pp. 12007–12013, 2012.
- [32] Z. R. Kann and J. L. Skinner, "Self-diffusion and viscosity in electrolyte solutions," *Journal of Chemical Physics*, vol. 141, no. 7, p. 104507, 2014.
- [33] C. J. Tainter, P. A. Pieniazek, Y.-S. Lin, and J. L. Skinner, "Robust three-body water simulation model" *Journal of Chemical Physics*, vol. 134, no. 7, p. 184501, 2011.